Title

THERMAL FRAGMENTATION OF ETHYLENE ON THE RH(100) SINGLE CRYSTAL SURFACE IN THE TEMPERATURE RANGE OF 200-800 K

Authors

Slavin, A.J.
Bent, B.E.
Kao, C.T.

Publication Date

1988-04-01

LBL-24757
Preprint

Center for Advanced Materials

CAM

Submitted to Surface Science

Thermal Fragmentation of Ethylene on the Rh(100) Single Crystal Surface in the Temperature Range of 200–800 K

A.J. Slavin, B.E. Bent, C.-T. Kao, and G.A. Somorjai

April 1988

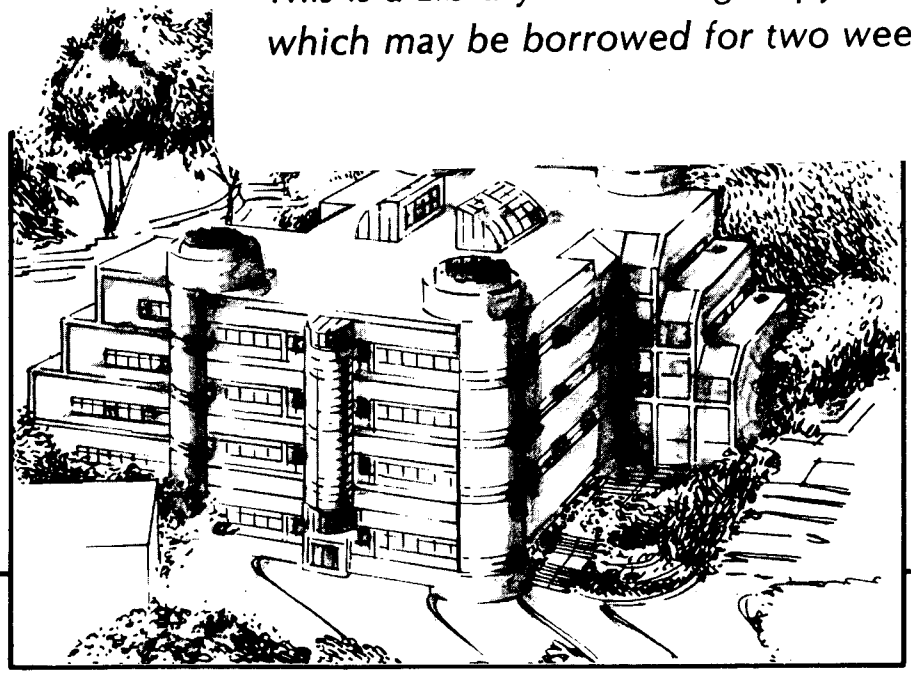

Materials and Chemical Sciences Division

Lawrence Berkeley Laboratory • University of California

ONE CYCLOTRON ROAD, BERKELEY, CA 94720 • (415) 486-4755

Prepared for the U.S. Department of Energy under Contract DE-AC03-76SF00098

DISCLAIMER

LBL 24757

Thermal Fragmentation of Ethylene on the Rh(100) Single Crystal Surface in the Temperature Range of 200 - 800 K

A.J. Slavin*, B.E. Bent**, C-T Kao and G.A. Somorjai

Materials and Chemical Sciences Division
Lawrence Berkeley Laboratory
and
Department of Chemistry
University of California
Berkeley, California 94720
U.S.A.

*Present Address: Dept. of Physics, Trent University, Peterborough, Ontario K9J 7B8 Canada

**Present Address: AT&T Bell Laboratories, Murray Hill, NJ 07974, U.S.A.

ABSTRACT

High resolution electron energy loss spectroscopy (HREELS), low-energy electron diffraction (LEED), and thermal desorption spectroscopy (TDS) have been utilized to study the thermal fragmentation chemistry of ethylene between 200 and 800 K on a Rh(100) surface. We find that the kinetically stable decomposition intermediates vary with surface coverage. At room termperature and adsorbate coverages less than θ=0.5, ethylene dehydrogenates to CCH; ethylene adsorbed in excess of θ=0.5 is converted instead to CCH_3. The CCH_3 (ethylidyne) is thermally stable up to 380 K, while the CCH species remain intact up to ~450 K. The complexity of the HREEL spectra for the decomposition of CCH_3 and CCH in the temperature range of 380-800 K suggests that a mixture of surface fragments is present. There is some evidence that CCH_2, which is stable between 380 and 400 K, is formed during ethylidyne decomposition. We compare our results here with those for ethylene decomposition on other transition metal surfaces and suggest a reaction sequence involving elementary hydrogenation and dehydrogenation reactions to explain the surface chemistry.

1. INTRODUCTION

The effects of the geometrical arrangement of surface atoms on the bonding and catalytic chemistry of hydrocarbons over transition metal catalysts vary depending on the hydrocarbon and the reaction. For example, it has been found that the rates and selectivities of catalytic hydrocarbon reactions such as isobutane and n-butane isomerization are strongly dependent on metal surrace structure [1]. One the other hand, catalytic n-hexane isomerization is reported to be a relatively "structure insensitive" reaction [2]. It appears that a similar dichotomy may also exist for the stoichiometric chemistry of hydrocarbons on single crystal transition metal surraces. For example, the bonding and thermal decomposition pathways for ethylene on Pd(111) [3] and Pd(100) [4] surfaces in ultra-high vacuum (UHV) are substantially different, while benzene adsorption on these same surfaces [5] seems relatively structure insensitive.

In order to see if ethylene shows structure sensitive chemistry in general on face-centered cubic (111) vs. (100) surfaces, while benzene does not, we have recently studied the thermal chemistry of ethylene and benzene on a Rh(100) surface in UHV to compare with previously published results for these molecules on the Rh(111) surface [ethylene:6-10, benzene: 11,12]. We report here studies of ethylene thermal decomposition on Rh(100) in the temperature range of 200-800 K. These studies supplement earlier publications on the low temperature adsorption of molecular ethylene on Rh(100) [10] and the room temperature coadsorption of ethylene with carbon monoxide on Rh(100) to form ethylidyne (CCH_3) [13]. In the present study, low-energy electron diffraction (LEED), high-resolution electron energy loss spectroscopy (HREELS), and thermal desorption spectroscopy (TDS) were used to investigate the surface chemistry. We find that, in comparison to Rh(111), the chemistry of ethylene on Rh(100) can be viewed as both

structure sensitive and structure insensitive depending on the surface coverage. For low coverages of ethylene on Rh(100) ($\Theta_{C_2H_4}$>0.5), the first stable decomposition fragment is C_2H in contrast to the CCH_3 species found on Rh(111). At higher surface coverages this structure sensitivity disappears and the thermal chemistry of ethylene adsorbed in excess of half a monolayer on Rh(100) is quite similar to the coverage-independent chemistry of ethylene on Rh(111). We also compare the ethylene/Rh(100) chemistry with ethylene decomposition on other transition metal surfaces, and an explanation for the C-H bond chemistry observed in terms of elementary hydrogenation and dehydrogenation steps is suggested.

2. EXPERIMENTAL

The experiments were carried out in a UHV chamber with a base pressure of 2×10^{-10} Torr equipped for Auger electron spectroscopy (AES), LEED, HREELS, and TDS. The chamber, sample cleaning procedure, and other experimental details have been discussed thoroughly elsewhere [8]. The HREEL spectrometer consisted of 127^{o} cylindrical monochromator and analyzer sector. The total scattering angle was fixed at 120^{o}. For all the specular HREEL spectra, the angle of incidence was set at 60^{o}. The resolution was 6.3-7.5 meV (50-60 cm^{-1}, 1 meV=8.0655 cm^{-1}) and the beam energy 2-4 eV. The HREEL spectra reported here were recorded at 100 K, or 300 K after momentarily warming to the temperatures indicated on the spectra, unless noted otherwise.

3. RESULTS AND INTERPRETATION

We present first our LEED and HREELS results on the decomposition of ethylene on Rh(100) at surface temperature between 200-380 K. Subsequent decomposition of these room temperature fragments at elevated temperatures up to 800 K is then discussed, followed by a comparison with TDS studies.

3.1 Decomposition in the Temperature Range of 200-380 K

Figure 1 shows HREEL spectra for the decomposition of saturation coverages of C_2H_4 and C_2D_4 on Rh(100) at approximately room

temperature. All three monolayers showed c(2x2) LEED patterns. The monolayers in Fig. 1a and 1b are both the result of C_2H_4 adsorption, but in 1a, the ethylene was adsorbed at 210 K followed by warming to 273 K with the spectrum taken at 273 K; in 1b, the ethylene was adsorbed at a surface temperature of 310 K. The peak at 1825 cm^{-1} in 1a is from CO, presumably adsorbed during cooling to 210 K. The slightly different peak frequencies and intensities of the remaining peaks in these two spectra are indicative of the variation we observed in the saturation coverage HREEL spectra. This variability is not due to the different temperatures at which the spectra were taken (both monolayers in Fig. 1a and 1b are thermally stable up to 380 K), but is instead probably due to the complexity of ethylene decomposition on Rh(100). In particular, we have found that the ethylene decomposition pathway on Rh(100) is coverage dependent and highly sensitive to low levels of contamination. Also, there is no a priori reason why an ethylene molecule incident on a surface at a given temperature should produce the same fragments generated by a condensed layer of ethylene warmed to the same temperature.

Assignment of the complex HREEL spectra in Figure 1 is facilitated by looking first at the low coverage ethylene vibrational spectra. Figure 2 shows specular HREEL spectra for subsaturation coverages of C_2H_4 and C_2D_4 adsorbed on Rh(100) at 325 K. Figures 2b and 2c are for 1.0 L (1 Langmuir = 10^{-6} torr-sec) of ethylene and perdeuteroethylene respectively; both of these adsorbed layers showed a c(2x2) LEED pattern. The lower coverage 0.5L spectrum for C_2H_4 in Fig. 2a shows a p(2x2) LEED pattern, but the vibrational features are quite similar to those for the higher coverage c(2x2) structure in Fig. 2b. The major features in the hydrogenated spectra are two low-frequency modes at 350-450 cm^{-1}, a peak at 800-850 cm^{-1}, a weak mode at 1300-1350 cm^{-1}, and a peak at >3000 cm^{-1}. The peaks at 1775-1950 cm^{-1} in Fig. 1 and 2 are due to C-O stretch of carbon monoxide from background adsorption. The surface concentration of such contaminated species was estimated to be less than 0.07 monolayer coverage [14,15], and the shoulder at 680 cm^{-1} we suspect is due to some contaminate hydroxyl species [16].

The low frequency modes at 350-450 cm^{-1} are in the expected frequency range for metal-adsorbate vibrations. They may be partially

attributable to the contaminate CO, but their relative intensity is much larger than is observed for a comparable coverage of CO on a clean Rh(100) surface [14,15]. We conclude that these modes are due primarily to metal-hydrocarbon fragment vibrations. Of the other hydrocarbon fragment peaks, the modes at ~800 and ~3050 cm^{-1} are readily attributable to CH bend and stretch motions respectively based on their shift down in frequency by factors of 1.2-1.3 in the deuterated spectrum of Fig. 2c. The weak, broad feature at 1300-1350 cm^{-1} in the hydrogenated spectra can be correlated with the 1280 cm^{-1} mode in the deuterated spectrum. We assign this peak to a C-C stretching vibration based on the small frequency shift with deuteration. The presence of this νCC mode indicates that the C-C bond remains intact when ethylene is adsorbed on Rh(100) at room temperature. We leave the broad hump at 905 cm^{-1} in the deuterated spectrum unassigned; it may be due to contamination.

The observed low coverage modes for ethylene adsorbed at room temperature are consistent with $C_2H(C_2D)$. This surface species account for the observed C-C stretch mode and the lone CH(CD) bend and stretch modes. Species with CH_2 and CH_3 groups can be discounted based on the absence of CH_x deformation modes in the 1300-1450 cm^{-1} region. In Table 1 we sumarize our assignment of the spectra in Fig. 2 to this C_2H species. This assignment is compared with previous HREEL spectral assignments of C_2H species on Rh(111) [17], Pd(111) [18], Pd(100) [18], Ni(110) [19], and Ru(001) [20] as well as with infrared frequencies for a C_2H ligand coordinated to three osmium atoms in an organometallic cluster [21]. Consistent with the low νCC frequency of 1534 cm^{-1} in the cluster, the νCC mode in C_2H on these transition metal surfaces is shifted down by hundreds of cm^{-1} from the frequency for a gas phase carbon-carbon triple bond of 1974 cm^{-1} [22]. This large frequency shift can be attributed to a bonding configuration of C_2H where the C-C bond interacts with several metal

atoms as is found for the triosmium complex [21]. While the triosmium complex is a poor structural model for a tilted C_2H species on a Rh(100) surface, there is a pentaruthenium complex in which a C_2(phenyl) ligand interacts directly with four metal atoms analogous to bonding in a 4-fold hollow site on Rh(100). The bonding geometry of this complex [23] along with its analogue for a Rh(100) surface are shown in Fig. 3. The νCC vibrational frequency for the pentaruthenium complex has not been reported, but such a tilted geometry can account for both the low frequency and weak spectral intensity of the νCC mode on Rh(100).

The saturation coverage HREEL spectra in Fig. 1 are quite different from the low coverage acetylide spectra in Fig. 2. The most distinctive additional modes in the hydrogenated spectra of Fig. 1 are: (1) a lower frequency νCH peak at ~2900 cm^{-1}, (2) an intense mode at 1330 cm^{-1}, (3) a peak at 970-1020 cm^{-1}, and (4) a shoulder at 700-750 cm^{-1}. The peak at 1330 cm^{-1} which shifts down with deuteration is characteristic of a methyl group, as is the 2900 cm^{-1} CH_x peak. Similar frequencies (with the exception of the 700-750 cm^{-1} peak) and relative intensities were reported previously [13], as reproduced in fig. 5a, for adsorption of ethylene on a Rh(100) surface precovered with a half monolayer of carbon monoxide. In that work, these peaks were assigned to ethylidyne (CCH_3) species on the surface. It seems probable that the half monolayer [24] of adsorbed C_2H that forms for low coverages of adsorbed ethylene, may be directing subsequently adsorbed ethylene in excess of half a monolayer to form ethylidyne analogous to the effect of preadsorbed CO. We therefore attribute the spectra in Fig. 1 to a mixture of C_2H and CCH_3 species on Rh(100). The C_2H peaks have been assigned in Table 1. The ethylidyne peaks are assigned based on ref. 13 as follows (deuterated frequencies in parenthesis): 2890 (2130) = νCH_3, 1330(930) = $\delta_s CH_3$ and ~1000(1055) = νCC. We note that other fragments such as CCH_2 may also be present as minority species. The presence of such a fragment

could account for the unassigned modes at 700-740 cm^{-1} and at 1135 cm^{-1} in the hydrogenated spectra.

3.2 Decomposition Above 380 K

The HREEL spectra for thermal decomposition of a CCH_3 + CCH monolayer above 380 K on Rh(100) are shown in Fig.4. Most of the features in these spectra are attributable to the decomposition of CCH_3 on Rh(100). The CCH species, in addition to having relatively few vibrational modes, is already highly dehydrogenated, and further dehydrogenation leads to surface carbon which has no sharp vibrational modes on Rh(100).

The HREEL spectra for decomposition of CCH_3 in the absence of CCH but coadsorbed with CO are shown in Fig. 5; they are indeed quite similar to those spectra with CCH present in Fig. 4. The starting monolayer of CCH_3 in Fig. 5a was prepared by coadsorption of ethylene and carbon monoxide [13]: first 0.7 L of CO was adsorbed to give a c(2x2) LEED pattern, followed by adsorption of 160 L of ethylene at 300 K. We suspect that the differences in the peak frequencies and intensities in the 380 and 520 K spectra of Fig. 5 in comparison with the analogous monolayers in Fig. 4 are due to varying degrees of dehydrogenation (there is continuous hydrogen evolution from the surface from 380-700 K) rather than to the effects of CO vs. CCH on CCH_3 decomposition.

The complex HREEL spectra in Fig. 5 for ethylidyne decomposition above 380 K on Rh(100) cannot be definitively assigned. Probably a mixture of surface species is present on the surface at these elevated temperatures. We can say that ethylidyne begins to decompose at about 380 K on Rh(100), since in the 380 K spectrum for CCH_3 + CO decomposition in Fig. 5b, all the ethylidyne modes have essentially disappeared. The 380 K spectrum for CCH_3 + CCH decomposition in

Fig. 4b still shows some ethylidyne based on the presence of the 1325 cm^{-1} peak, but the changes in the lower frequency modes and the appearance of the 1420 cm^{-1} peak indicate significant decomposition.

A chemically reasonable explanation for the complex spectra in Figs. 4b and 5b is that the major decomposition product from CCH_3 is CCH_2. Other more highly dehydrogenated species (even mixtures of species) would be too vibrationally simple to account for the many modes observed [25]. Based on the published spectra of surface [26] and cluster [27] bound CCH_2 species, this ligand is expected to have multiple vibrational peaks in the 800-1450 cm^{-1} region. Also, since this ligand is expected from organometallic chemistry to bond with a tilted geometry on a clean transition metal surface [26,27], the highest possible adsorption symmetry on Rh(100) is C_s. This low adsorption symmetry means that most of the vibrational modes will be dipole active [28] which can account for some of the complexity in Figs. 4b and 5b.

The ethylene decomposition spectra above 380 K on Rh(100) show qualitatively the same features found for high temperature decomposition of unsaturated hydrocarbons on a number of transition metal surfaces, including Rh(111) [12,17], Pt(111) [29], Ni(111) [30], and Ru(001)[20]. These spectra have been attributed to polymeric C_xH species [12,17] or CH species [20,29,30]. In each of these cases, the mode at 700-850 cm^{-1} is assigned to a CH bend and/or metal-carbon stretch, while the peak at ~3000 cm^{-1} is assigned to a CH stretch. The blob at ~1300 cm^{-1} has been attributed to C-C stretching modes in polymeric species. We know of no satisfactory explanation of the mode frequently observed at ~1150 cm^{-1} or for why the observed νCH frequency shifts down below 3000 cm^{-1} just prior to complete dehydrogenation [12] as seen in Fig. 4d.

3.3 Thermal Desorption Spectroscopy

Hydrogen thermal desorption spectra for ethylene adsorption on Rh(100) are difficult to interpret both because of the coverage dependence of the surface decomposition pathway and because several dehydrogenation reactions occur at or below the temperature where surface hydrogen atoms recombine and desorb. The thermal desorption spectra can, however, provide some support for our interpretations above of the HREEL spectra.

Hydrogen TD spectra for ethylene adsorbed at <150 K on Rh(100) are shown in Fig. 6. The absence of hydrogen desorption below 200 K is consistent with the observation that C_2H_4 adsorbs without dissociation in this temperature regime [10]. Also shown in the mass 27 desorption for a saturation exposure of ethylene. Because of the low peak temperature (155 K) [31] and the broadness of this peak, we atttribute this m/e = 27 spectrum to desoprtion from the Ta support wires. The 0.25 and 0.5 L H_2 TD spectra in Fig. 6 are consistent with CCH formation and decomposition. The first peak at 300-400 K is due to desoprtion of surface hydrogen produced in the foramtion of CCH below room temperature. The 450 K peak is then a result of CCH dehydrogenation. The integrated ratio fo these 350 and 480 K peaks (2.8:1) is consistent with the stoichiometry of CCH species to within the ~10% uncertainty of TDS.

The higher exposure TDS in Fig. 6 are more complex because both CCH_3 and CCH species form. It is interesting but not understood why a lower temperature H_2 desorption peak appears at 250 K for higher ethylene exposures. Presumably both this 250 K peak and the 325 K peak are due to desorption of hydrogen bound to the Rh(100) surface. These peaks are absent for ethylene adsorptions at 300 K.

The origin of the 250 K peak is unclear. It may be due to a second surface state for hydrogen, although no such peak has been seen from the adsorption of hydrogen alone [15,52]. Alternatively, it might result from direct emission of hydrogen from dehydrogenation once the available surface has become saturated with hydrogen. This would, of course, require the saturated surface to act as the catalyst for dehydrogenation.

Attempts to investigate the source of the 250 K TDS peak more closely, by taking HREEL spectra near 273 K following dosing at 210 K, were largely uncussessful. The result for a 5 L dose was given in fig. 1a and has been discussed previously. Results for doses of 1 L or less were irreproducible because of surface contamination occurring while the spectra were being taken. The TDS spectra at these low coverages were, however, very reproducible and are believed to reflect accurately the hydrocartbon decomposition.

The H_2 TDS for CCH_3 in the absence of CCH and adsorbed hydrogen atoms has been published [13]. In that spectrum, a peak is clearly observed at 385 K. According to our HREELS analysis (fig. 5b), this peak can be attributed to conversion of CCH_3 to CCH_2 with subsequent conversion to CCH. The desorption tail at still higher temperature then represents dehydrogenation and polymerization of C_xH species.

4. DISCUSSION

4.1 Thermal Decomposition of Ethylene on Rh(100) and Comparison to Rh(111)

Our HREEL spectroscopy studies here clearly show that the kinetically stable intermediates formed during ethylene decomposition on

Rh(100) change with coverage. For coverages less than $\Theta = 0.5$, the stable decomposition intermediate at room temperature is C_2H. At higher ethylene exposures, the stable room temperature decomposition fragment is CCH_3 (ethylidyne) rather than C_2H. These ethylidyne species begin to decompose at 380 K on Rh(100), while the CCH species are stable above 400 K. Our HREELS studies suggest that ethylidyne deocomposes on Rh(100) to give predominantly CCH_2 species, but other more highly dehydrogenated fragments are probably also present. All of these partially hydrogenated fragments on Rh(100) decompose above 500 K to give a monolayer attributed to a mixture of CH and/or polymeric C_xH species.

The thermal chemistry of ethylene and of ethylene coadsorbed with carbon monoxide on Rh(100) is summarized and compared to that for ethylene on Rh(111) in Fig. 7. Probably the most significant difference in the thermal fragmentation of ethylene on these surfaces is the coverage dependence of the chemistry on Rh(100) versus the coverage independence found on Rh(111). At room temperature and coverages less the $\Theta = 0.5$, dehydrogenation is more extensive on Rh(100) than on Rh(111). At higher coverages, this enhanced dehydrogenation on Rh(100) is suppressed and the decomposition fragments on the two surfaces are quite similar.

It is interesting that a half monolayer of either CO or CCH species prevents the room temperature decomposition of ethylene to CCH on Rh(100). Further, preliminary studies indicate that a half monolayer of carbon or of sulfur atoms also has a similar effect on ethylene decomposition on Rh(100). Since CO bonds in top and bridge sites on Clean Rh(100) [14,15], while sulfur [32] (and possibly carbon [33] and CCH [34]) bonds in 4-fold hollow site, decomposition of ethylene to CCH probably involves a small ensemble of sites rather than a specific site.

Based on the fact that the coverage of these adsorbates must by Θ_{ads} = 0.5 before CCH formation is completely blocked, the ensemble size is between 2 and 4 metal atoms. Also, since similar decomposition to CCH does not occur on Rh(111) at room temperature, the ensemble probably requires at least one 4-fold hollow site. It is not yet clear whether ethylidyne is an intermediate in CCH formation and is only kinetically stable on Rh(100) at high adsorbate coverages or whether two different decomposition pathways occur - one that produces CCH at low coverage and another which produces CCH_3 at high coverage.

4.2 General Aspects of Ethylene Adsorption and Fragmentation on Transition Metal Surfaces

Almost all the information reported to date on the identity of ethylene and its thermal decomposition fragments on transition metal surfaces has come from HREELS and TDS. Also, except for a few studies on the group 6 metals, almost all data for ethylene fragmentation has been obtained for group VIII B metals. Thus, only these metals will be discussed here.

Figs. 8 and 9 show the thermal reaction pathways that have been identified for ethylene on the 3d and 4d/5d metal surfaces respectively [35]. The experimental results are so grouped because the 3d metal surfaces appear to have chemistry more similar to one another than to the 4d or 5d metal surfaces of the same group in the periodic table. For example, on all the 4d and 5d metal surfaces in Fig. 9 except for Pd(100), at least one of the decomposition fragments is CCH_3. None of the 3d metal surfaces shown in Fig. 8 form this species [40]. Similar dichotomies between the 3d and 4d/5d metals in group VIII B also exist in molecular and solid state chemistry; e.g., in the crystal structure and lattice constant of the pure metals [41], the formation of simple hydrated ions [42], and the formation of high oxidation states [42].

On most of the group VIII B metal surfaces studied, the majority of adsorbed ethylene is irreversibly adsorbed and decomposes as shown in Figs. 8 and 9 through a number of identifiable partially hydrogenated fragments over the temperature range of 200-800 K. On both the 3d and 4d/5d metal surfaces (except possibly the highly corrugated Fe(111) surface), carbon-hydrogen bond breaking in ethylene occurs at lower temperatures than carbon-carbon bond breaking. C-H bond breaking generally begins betwen 200 and 300 K, while C-C bond breaking (except on Fe(111) and stepped Ni[5(111) x (110)] occurs above 300 K if at all. Since C-H bond breaking occurs at lower temperatures than C-C bond breaking and since all of the stable decomposition intermediates in Figs. 8 and 9 are more highly dehydrogenated than ethylene, it is generally assumed that ethylene fragmentation is initiated by C-H bond cleavage. Decomposition pathways initiated by partial hydrogenation of C_2H_4 to C_2H_5 are also possible, but have not been generally considered [43]. We discuss here the evidence for this latter decomposition pathway and show how decomposition initiated by partial hydrogenation of ethylene to ethyl species can help account for the observed decomposition products of ethylene on the group VIII B transition metals.

Based on the decomposition intermediates identified (Figs. 8 and 9), it appears that dehydrogenation is generally thermodynamically favored over hydrogenation on clean transition metal surfaces in ultra-high vacuum. There is, however, indirect evidence that ethylene can be hydrogenated to ethyl species on some of these surfaces at temperatures below where dehydrogenation of ethylene occurs. For example, ethane (C_2H_6) desorbs from Pt(111) at <270 K when ethylene is adsorbed in the presence of surface hydrogen atoms [44]. Surface ethyl species are presumably the intermediates in this hydrogenation. The presence of reversibly formed surface ethyl species could also explain the low temperature H,D exchange observed in ethylene on Pt(111) [45].

The potential role of ethyl species in ethylene decomposition on transition metal surfaces is intriguing, since by subsequent sequential dehydrogenation of these species one can account for all possible dehydrogenation products observed for ethylene. These possibilities are shown in Fig. 10. Such a scheme is an attractive explanation for the surface chemistry for several reasons as discussed below.

First, the elementary reactions in Figure 10 all have a strong chemical precedent. Reversible hydrogenation and dehydrogenation of ethylene has long been postulated to explain the catalytic H,D exchange in ethylene over group VIII B transition metal catalysts [46]. Similarly, reductive eliminations (hydrogenations) and oxidative additions (dehydrogenations) are well-documented in solution organometallic chemistry [47], and their applicability to the surface reactions of adsorbed hydrocarbons has been discussed [48]. Other possible mechanistic explanations for ethylene thermal chemistry such as intramolecular hydrogen shifts seem less likely in vacuum. In fact, recent molecular orbital calculations suggest that formal hydrogen transfer processses in hydrocarbon ligands on Pt(111) occur with significantly lower energy when they proceed via H transfer to the surface versus an intramolecular hydrogen shift [49].

Second, the reaction schemes in Fig. 10 provide reasonable explanations for a number of experimental observations. For example, it has been pointed out that the formation of ethylidyne (CCH_3) by first hydrogenationg C_2H_4 to C_2H_5 as shown in Fig. 10 can explain why ethylidyne forms on surfaces of those metals which are most active in catalytic ethylene hydrogenation [50]. The mechanistic sequence in Fig. 10 also provides a rationalization for the coverage dependent chemistry of ethylene on Rh(100) and for similar chemistry observed on Ru(001) [20,51]. In particular, it may be that the conversion of ethylene to CCH at low coverages versus CCH_3 at high coverages is due to two different

decomposition mechanisms - one initiated by dehydrogenation and favored by larger ensembles of metal atoms at low surface coverages and another initiated by hydrogenation and favored at high surface coverages where dehydrogenation is blocked.

Finally, we have found that the conceptual simplicity of the reaction sequences in Fig. 10 is useful for organizing and critically evaluating the rapidly accumulating literature on ethylene decomposition on transition metal surfaces.

5. CONCLUSIONS

We have shown, based on our HREELS results, that the thermal decomposition of ethylene on Rh(100) is coverage dependent. At 380 K and for coverages less then $\theta = 0.5$, ethylene dehydrogenates to CCH species; ethylene adsorbed in excess of $\theta = 0.5$ is converted to CCH_3 (ethylidyne) species.

The HREEL spectra for the subsequent decomposition of these species above 380 K are complex, suggesting that a mixture of surface species are present at all temperatures between 400 and 800 K. The spectra do provide some evidence that CCH_3 decomposes above 380 K predominantly to CCH_2 which subsequently dehydrogenate and polymerize to C_xH species. The high coverage fragments and their decomposition temperature for ethylene on Rh(100) are quite similar to the previously reported coverage-independent chemistry of ethylene on Rh(111); however, at low coverages, deydrogenation is much more extensive on Rh(100) than on Rh(111). These results, as well as those for ethylene decomposition on other transition metals, are rationalized using the reaction scheme shown in Fig. 10.

ACKNOWLEDGEMENTS

This work was supported by the Director, Office of Energy Research, Office of Basic Energy Sciences, Materials Sciences Division, U.S. Department of Energy under Contract Number DE-AC03-76SF00098. We thank Prof. J.R. Shapley for sending us infrared frequencies of the $Os_3(CO)_9(H)(CCH)$ cluster prior to publication. A.J. Slavin gratefully acknowledges support from the Natural Sciences and Engineering Research Council of Canada and the hospitality of the Berkeley laboratory; B.E. Bent gratefully acknowledges the National Science Foundation for a predoctoral fellowship; C.-T. Kao gratefully acknowledges a B.P.- America Fellowship for graduate research.

Table 1: Observed Vibrational Frequencies for C_2H Species

Mode Assignment	$Rh(100)/C_2H_4$[a] T = 300 K	$Os_3(CO)_9(\mu\text{-}H)(\mu_3\text{-}\eta^2\text{-}CCH)$[b]	$Rh(111)/C_3H_6$[c] T = 500 K	$Pd(111),(100)/C_2H_2$[d] T = 450 K	$Ni(110)/C_2H_4$[e] T = 300 K	$Ru(001)/C_2H_4$[f] T = 360 K
ν(CH)	3025(2290,1.32) [m]	3157(2377,1.33) [ms]	3020(2240,1.35) [m]	3000(2240,1.34) [m]	2990(2275,1.31) [m]	2960(2210,1.34) [m]
ν(CC)	1305(1280,1.02) [w]	1534(1496,1.03) [ms]	1380(1380,1.00)[w,br]	1340(1340,1.00)[w,br]	1290(1275,1.01)[m,br]	1290(1260,1.02) [m]
δ(CH)	805(660,1.22) [ms]	861(714,1.21)#[m] 854(709,1.20)#[m]	~815(~550,1.48)[s,br]	750(545,1.38) [s]	890(725,1.23) [s]	750(550,1.36) [ms]
δ(CH)	----	762(----) [w] 759(----) [w]	----	----	----	----
combination ν(MC)+δ(CH)	----	1259 (----) [m]	1170(----) [w]	----	----	----
ν_s(MC)	~430	----	490(----) [m]	----	465(445,1.04) [m]	435(----) [-]
ν_{as}(MC)	~370	----	----	----	380(360,1.06) [m]	----

Frequencies are in cm^{-1}; numbers in parenthesis are (frequencies for deuterated analogues, νCH/νCD)
s-strong, m-medium, w-weak, br-broad, #-doublets are reported by J.R. Shapley from spectra taken in a KBr pellet and are probably solid state splittings.

a) This work
b) Evans and McNulty, ref. 21, and J.R. Shapley, unpublished results
c) Bent et. al., ref. 17
d) Kesmodel et. al., ref. 18
e) Stroscio et.al., ref. 19
f) Hills et. al., ref. 20

REFERENCES

1. S.M. Davis, F. Zaera and G.A. Somorjai, J. Am. Chem. Soc. 104 (1982) 7453, and references therein.

2. S.M. Davis, F. Zaera and G.A. Somorjai, J. Catal. 85 (1984) 206, and references therein.

3. J.A. Gates and L.L. Kesmodel, Surf. Sci., 124 (1983) 68.

4. E.M. Stuve and R.J. Madix, J. Phys. Chem., 89 (1985) 105.

5. L.L. Kesmodel, Phys. Rev. Lett., 53 (1984) 1001; G.D.. Waddill and L.L. Kesmodel, Phys. Rev. B31 (1984) 4940.

6. L.H. Dubois, D.G. Castner and G.A. Somorjai, J. Chem. Phys., 72 (1980) 5234.

7. R.J. Koestner, M.A. Van Hove and G.A. Somorjai, Surf. Sci., 121 (1982) 321.

8. B.E. Koel, B.E. Bent and G.A. Somorjai, Surf. Sci., 146 (1984) 211.

9. B.E. Bent, Ph.D. Thesis, University of California, Berkeley (1986).

10. B.E. Bent, C.M. Mate, C-T. Kao, A.J. Slavin and G.A. Somorjai, submitted to J. Phys. Chem.

11. B.E. Koel, J.E. Crowell, C.M. Mate and G.A. Somorjai, J. Phys. Chem., 88 (1984) 1988.

12. B.E. Koel, J.E. Crowell, B.E. Bent, C.M. Mate and G.A. Somorjai, J. Phys. Chem., 90 (1986) 2949.

13. A.J. Slavin, B.E. Bent, C.-T. Kao and G.A. Somorjai, submitted to Surf. Sci.

14. L.H. Dubois, J. Chem. Phys., 77 (1982) 5228.

15. L.J. Richter, B.A. Gurney and W.Ho, J. Chem. Phys., 86 (1987) 477.

16. B.A. Gurney and W. Ho, J. Chem. Phys., 87 (1987) 1376.

17. B.E. Bent, C.M. Mate, J.E. Crowell, B.E. Koel and G.A. Somorjai, J. Phys. Chem., 91 (1987) 1493.

18. L.L. Kesmodel, G.D. Waddill and J.A. Gates, Surf. Sci., 138 (1984) 4464.

19. J.A. Stroscio, S.R. Bare and W. Ho, Surf. Sci., 148 (1984) 499.

20. M.M. Hills, J.E. Parmeter, C.B. Mullins and W.H. Weinberg, J. Am. Chem. Soc., 108 (1986) 3554.

21. J. Evans and G.S. McNulty, J. Chem. Soc., Dalton Trans. 79 (1984); J.R. Shapley, unpublished results.

22. T. Shimanouchi, Tables of Molecular Vibration Frequencies, Consolidated Volume I, NSRDS-NBS, 39 (1972) 51.

23. A.J. Carty, S.A. MacLaughlin and N.J. Taylor, J. Am. Chem. Soc., 103 (1981) 2456.

24. This surface coverage is presumed based on the c(2x2) LEED patterns observed for the C_2H and C_2D overlayers of Figs. 2B and 2C.

25. The observed modes in the 1300-1450 cm^{-1} range are almost certainly due to CH deformation modes in CH_2 and/or CH_3 groups. Carbon-carbon stretching modes are generally of weak intensity and modes for a CH group occur at lower frequency.

26. J.E. Parmeter, M.M. Hills and W.H. Weinberg, J. Am. Chem. Soc., 109 (1987) 72.

27. J. Evans and G.S. McNulty, J. Chem. Soc., Dalton Trans. (1983) 639.

28. Dipole active vibrational modes are generally observed in specular HREEL spectra. For a discussion of dipole scattering in HREELS, see H. Ibach and D.L. Mills, Electron Energy Loss Spectroscopy and Surface Vibrations, Academic, New York (1982).

29. A.M. Baro and H. Ibach, J. Chem. Phys., 74 (1981) 4194.

30. J.E. Demuth and H. Ibach, Surf. Sci., 78 (1978) 1238.

31. Molecular ethylene desorption from other group VIII B transition metal surfacs occurs above 200 K.

32. S. Hengrasmee, P.R. Watson, D.C. Frost and K.A.R. Mitchell, Surf. Sci., 87 (1979) L249.

33. The vibrational frequency of 555 cm^{-1} for carbon atoms on Rh(100) is almost exactly a factor of $(32/12)^{0.5}$ higher than that for sulfur atoms (313 cm^{-1}). This is expected in the harmonic oscillator approximation based on the mass difference and the assumption that the surface bond to these adsorbates has the same force constant. Therefore, since sulfur bonds in a 4-fold hollow, carbon may also.

34. See Fig. 3.

35. The decomposition pathways shown may be dramatically affected by the presence of coadsorbates. See for example ref. 36 and 51.

36. H. Steininger, H. Ibach and S. Lehwald, Surf. Sci., 117 (1982) 341.

37. U. Seip, M.-C. Tsai, J. Kuppers and G. Ertl, Surf. Sci., 147 (1984) 65.

38. W. Erley, A.M. Baro and H. Ibach, Surf. Sci., 120 (1982) 273.

39. S. Lehwald and H. Ibach, Surf. Sci., 89 (1979) 425.

40. Unpublished results of J. Eckerdt suggest that ethylidyne can be formed on a supported Ni catalyst from ethylene and hydrogen.

41. C. Kittel, Introduction to Solid State Physics, 5th Edition, New York, John Wiley, 74 (1976).

42. A.F. Wells, Structural Inorganic Chemistry, 3rd Edition, London, Oxford University Press, 907 (1962).

43. We note that only one H atom (from background gas or lower temperature fragmentation of some ethylene at surface imperfections) is needed, since subsequent dehydrogenation of C_2H_5 produces H-atoms to initiate the decomposition of other ethylene molecules.

44. D. Godbey, F. Zaera, R. Yeates and G.A. Somorjai, Surf. Sci., 167 1986) 150.

45. M. Salmeron and G.A. Somorjai, J. Phys. Chem., 80 (1982) 341.

46. J. Horiuti and K. Miyahara, "Hydrogenation of Ethylene on Metallic Catalysts," NSRDS-NBS, (1969) 13.

47. J.P. Collman and L.S. Hegedus, Principles and Applications of Organotransition Metal Chemistry, University Science Books, Mill Valley (1980).

48. E.L. Muetterties, Chem. Soc. Rev. 11 (1982) 283.

49. D.B. Kang and A.B. Anderson, Surf. Sci., 155 (1985) 639.

50. G.A. Somorjai, M.A. Van Hove and B.E. Bent, J. Phys. Chem., in press.

51. M.M. Hills, J.E. Parmeter and W.H. Weinberg, J. Am. Chem. Soc., 108 (1986) 7215.

52. Y. Kim, H.C. Peebles and J.M. White, Surf. Sci, 114 (1982) 363.

FIGURE CAPTIONS

Figure 1: Specular HREEL spectra of ethylene decomposition at ~300 K on a Rh(100) surface: (A) 5 L of ethylene dosed at 210 K and warmed to 273 K; spectrum recorded at 100 K, (B) 50 L of ethylene adsorbed at 310 K; spectrum recorded at 300 K, (C) deuterated analogue of spectrum in (B).

Figure 2: Specular HREEL spectra of ethylene decomposition on Rh(100) at 325 K and low coverage: (A) 0.5 L ethylene, (B) 1.0 L ethylene, (C) 1.0 L ethylene-d_4. All three monolayers formed ordered surface structures having the LEED patterns indicated. Spectra were recorded at 300 K.

Figure 3: (A) Proposed surface bonding of CCH on Rh(100) based on HREEL surface vibrational spectra and (B) the known bonding geometry for C_2(phenyl) in a pentaruthenium cluster [23].

Figure 4: Specular HREEL spectra of a Rh(100) surface after dosing 50 L of ethylene at 310 K followed by annealing to the indicated temperatures. All spectra were recorded at 300 K.

Figure 5: Specular HREEL spectra of a Rh(100) surface after dosing 0.7 L of CO followed ty 160 L of ethylene at 300 K and annealing to the indicated temperatures. The surface species in (A) are CO and ethylidyne (CCH_3) [13]. The surface fragments responsible for (B) and (C) are discusssed in the text. All spectra wre recorded at 300 K.

Figure 6: Amu=2 and amu=27 thermal desoprtion spectra for ethylene adsorbed on Rh(100) at 100 K. The molecular ethylene desorption (amu-27) at 155 K may originate from the crystal support wires (see text). The heating rates were 17 K/s.

Figure 7: Comparison of the thermal fragmentation pathways for ethylene adsorbed (with and without coadsorbed CO) on Rh(100) and Rh(111).

Figure 8: Thermal reaction pathways determined by TDS and HREELS for ethylene on 3d metal surfaces. Question marks indicate that the reaction pathway or surface species is uncertain. References: Fe(111) [37], Fe(110) [38], Ni(111) [39], Ni(110) [19], Ni[5(111)x(110)] [39].

Figure 9: Thermal reaction pathways determined by HREELS and TDS for ethylene adsorbed on 4d and 5d metal surfaces. Question marks indicate uncertain reaction pathways or surface species: References: Pt(111) [36], Rh(111) [9], Pd(111) [3], Ru(001) [20],, Rh(100) [this work], Pd(100) [4].

Figure 10: Proposed scheme for ethylene fragmentation on transition metal surfaces in the absence of C-C bond breaking. All the elementary steps are either hydrogenation (reductive elimination) or dehydrogenation (oxidative addition) reactions.

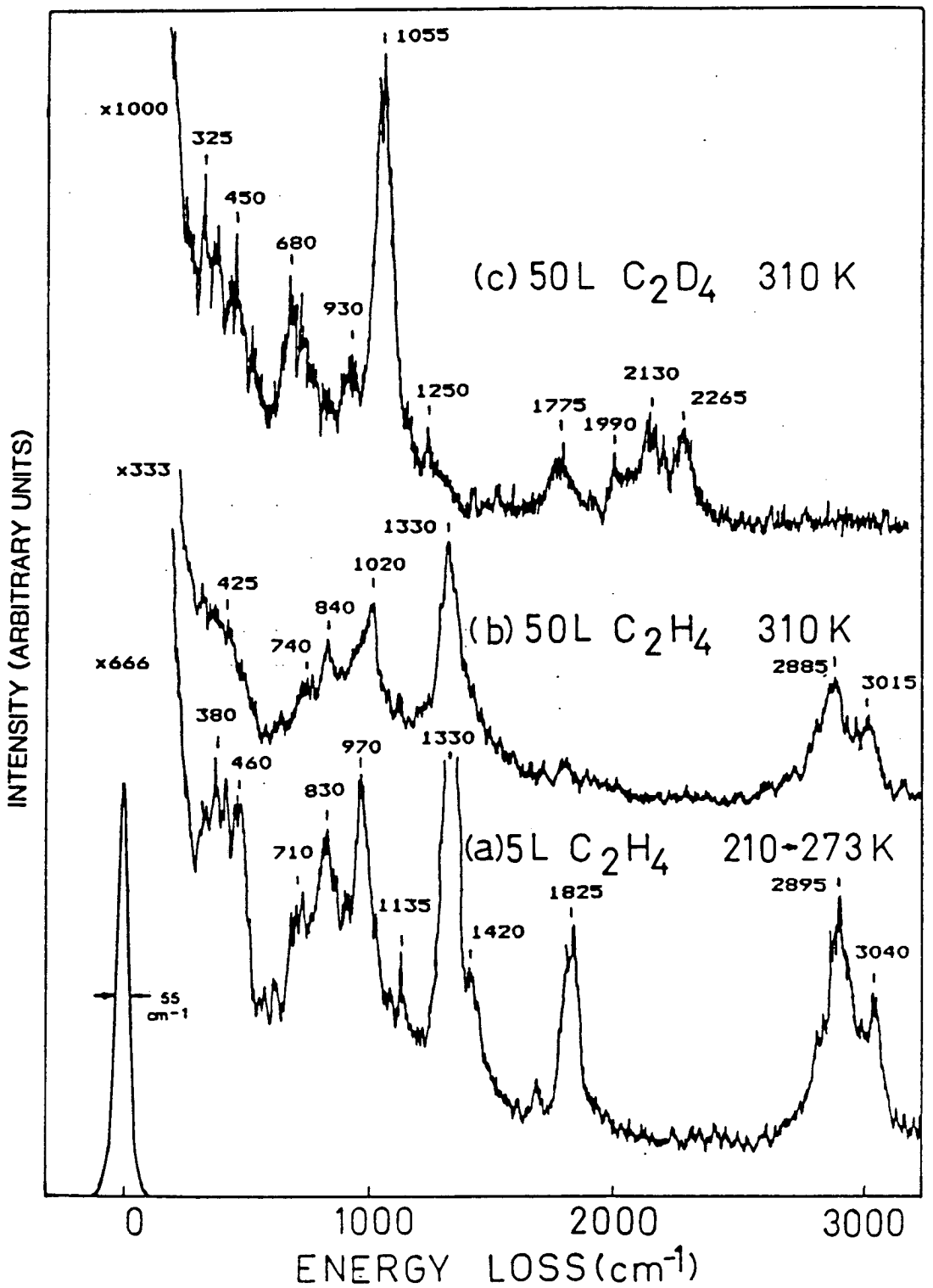

XBL 883-958

Figure 1

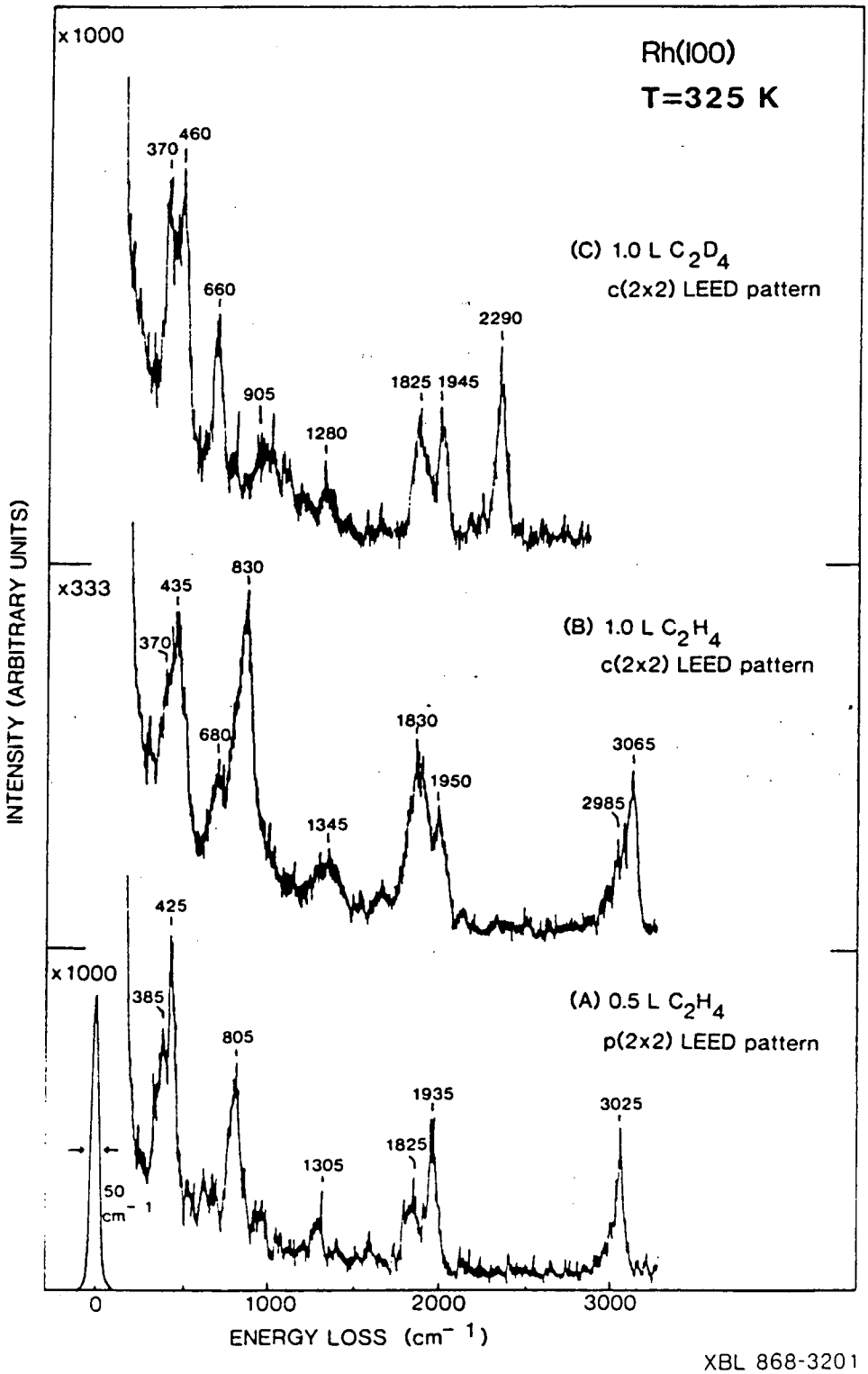

XBL 868-3201

Figure 2

(A)

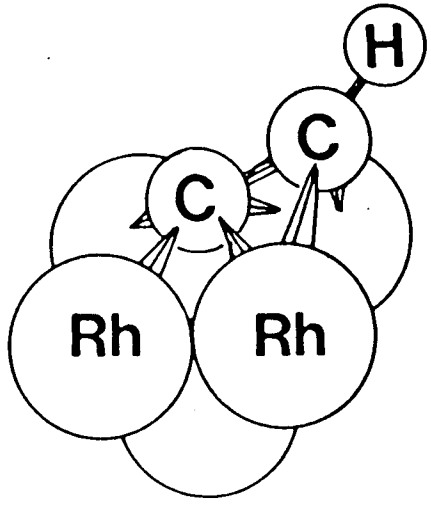

(B)

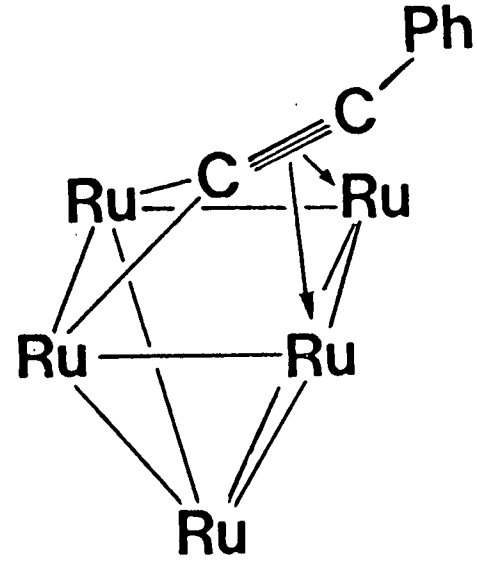

XBL 868-3191 A

Figure 3

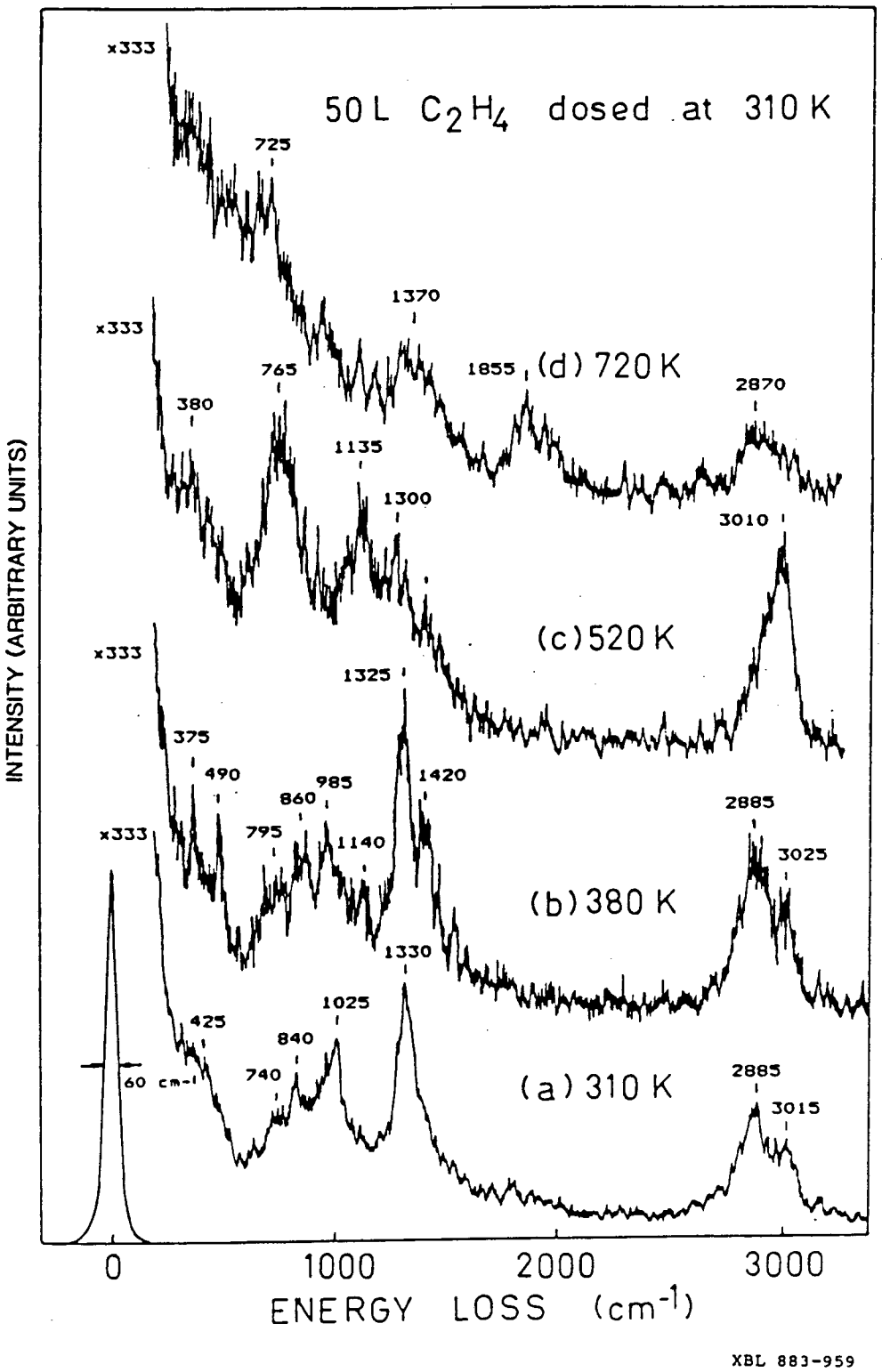
50 L C_2H_4 dosed at 310 K
(d) 720 K
(c) 520 K
(b) 380 K
(a) 310 K
x333
725
1370
1855
2870
765
380
1135
1300
3010
1325
375
490
985
860
1420
795
1140
2885
3025
1330
425
1025
840
740
2885
3015
60 cm-1
INTENSITY (ARBITRARY UNITS)
0
1000
2000
3000
ENERGY LOSS (cm^{-1})
XBL 883-959

Figure 4

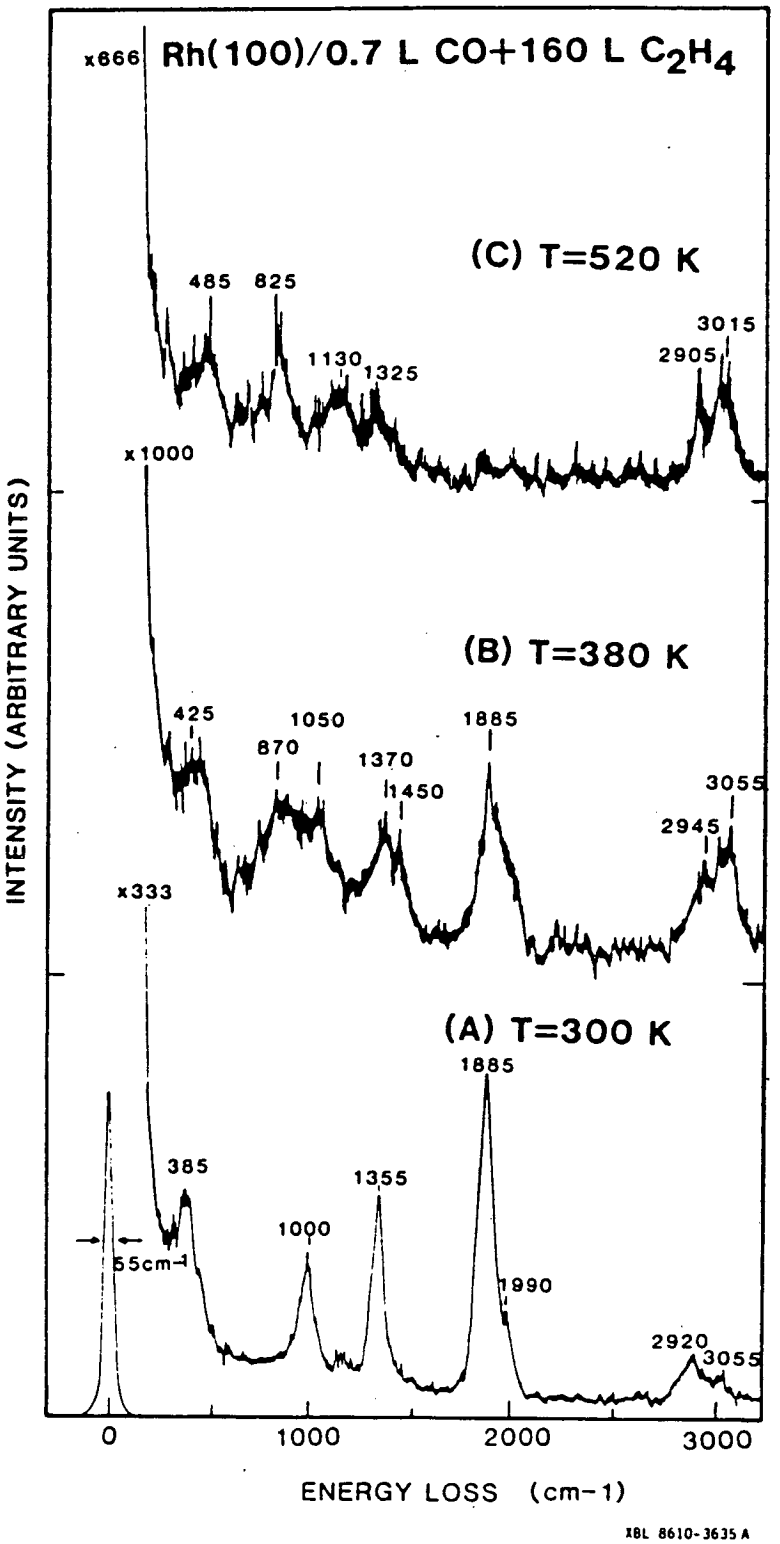
x666
Rh(100)/0.7 L CO+160 L C_2H_4
(C) T=520 K
485
825
1130
1325
2905
3015
x1000
(B) T=380 K
425
870
1050
1370
1450
1885
2945
3055
x333
(A) T=300 K
385
55cm-1
1000
1355
1885
1990
2920
3055
INTENSITY (ARBITRARY UNITS)
0
1000
2000
3000
ENERGY LOSS (cm-1)
XBL 8610-3635A

Figure 5

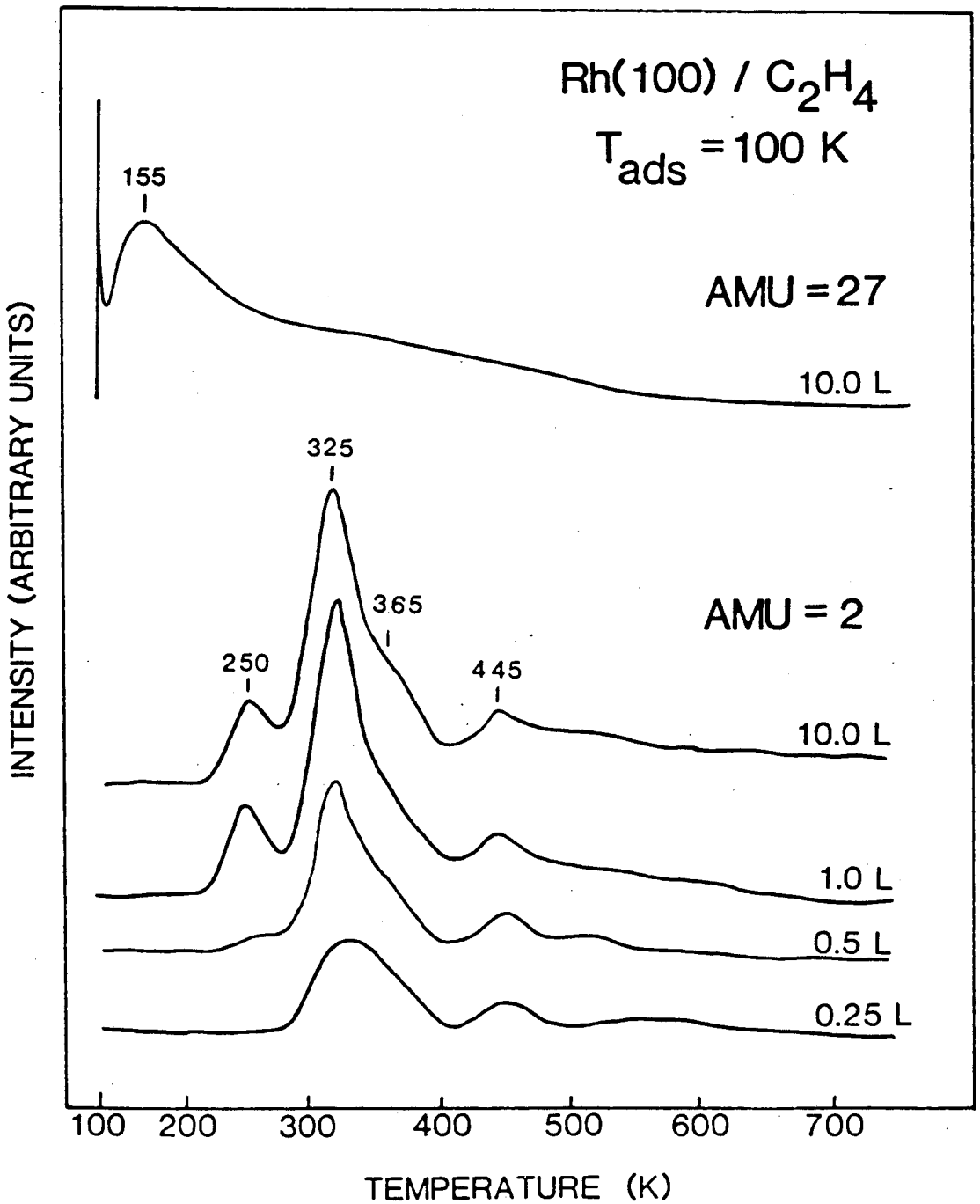

XBL 868-3199

Figure 6

(A) Rh(100)

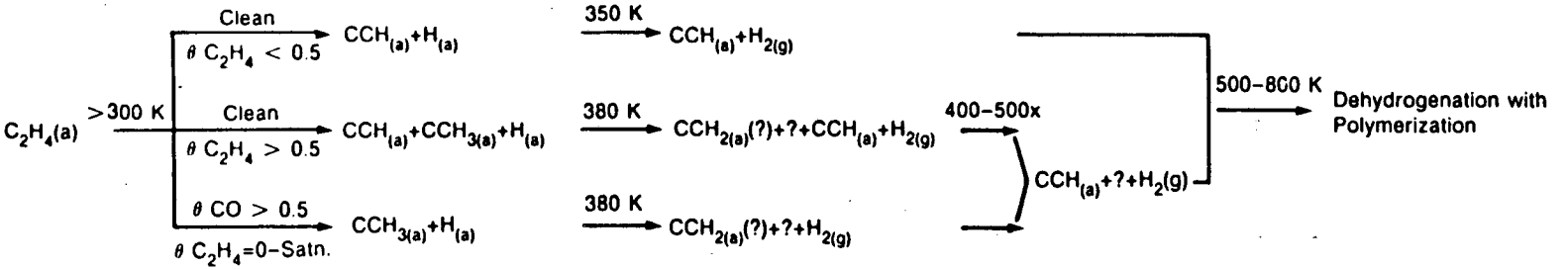

(B) Rh(111)

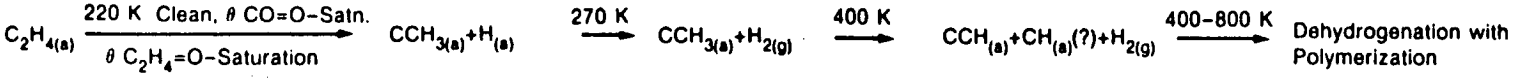

XBL 882-9563 A

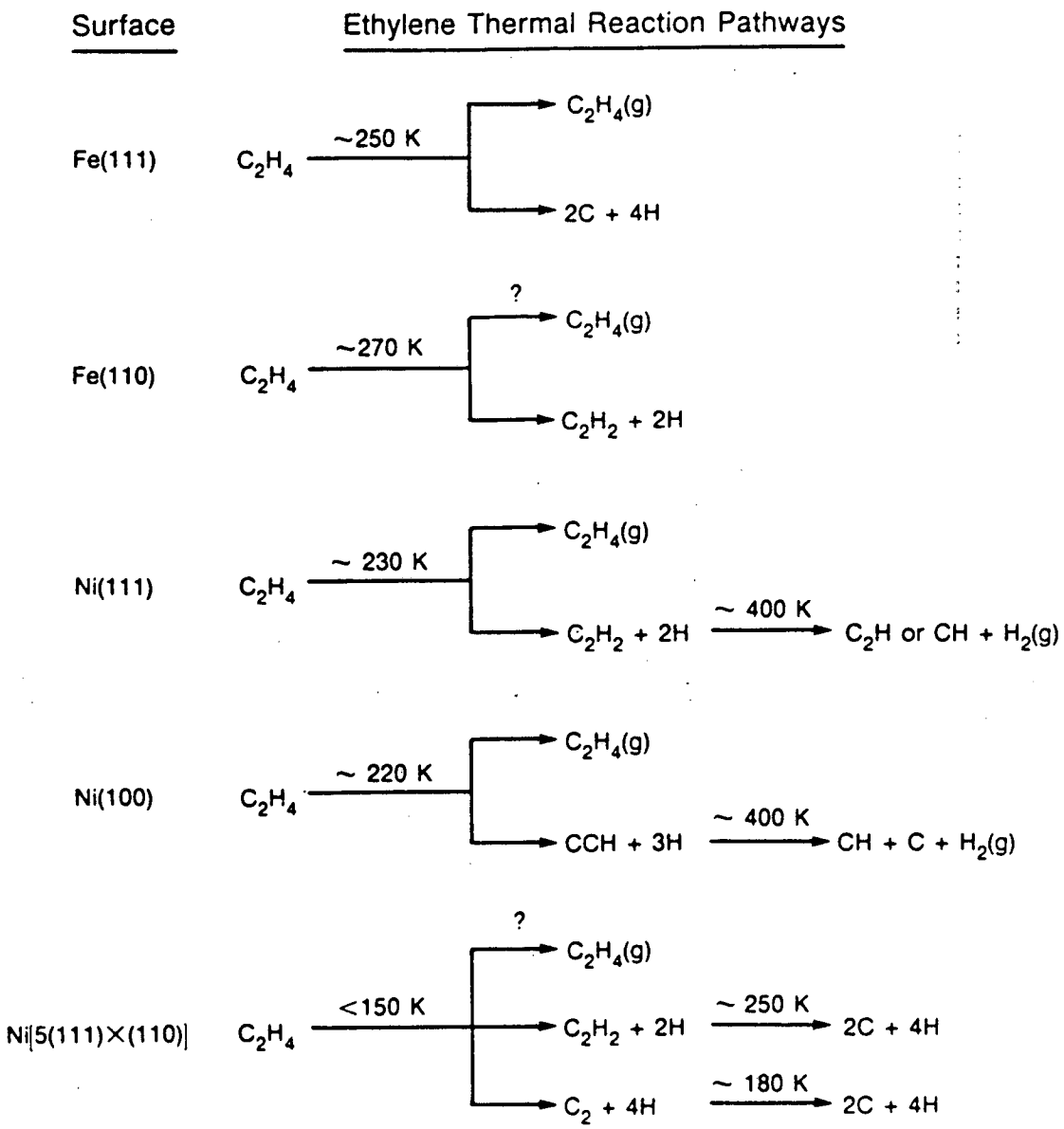

XBL 8610-4103

Surface	Ethylene Thermal Reaction Pathways

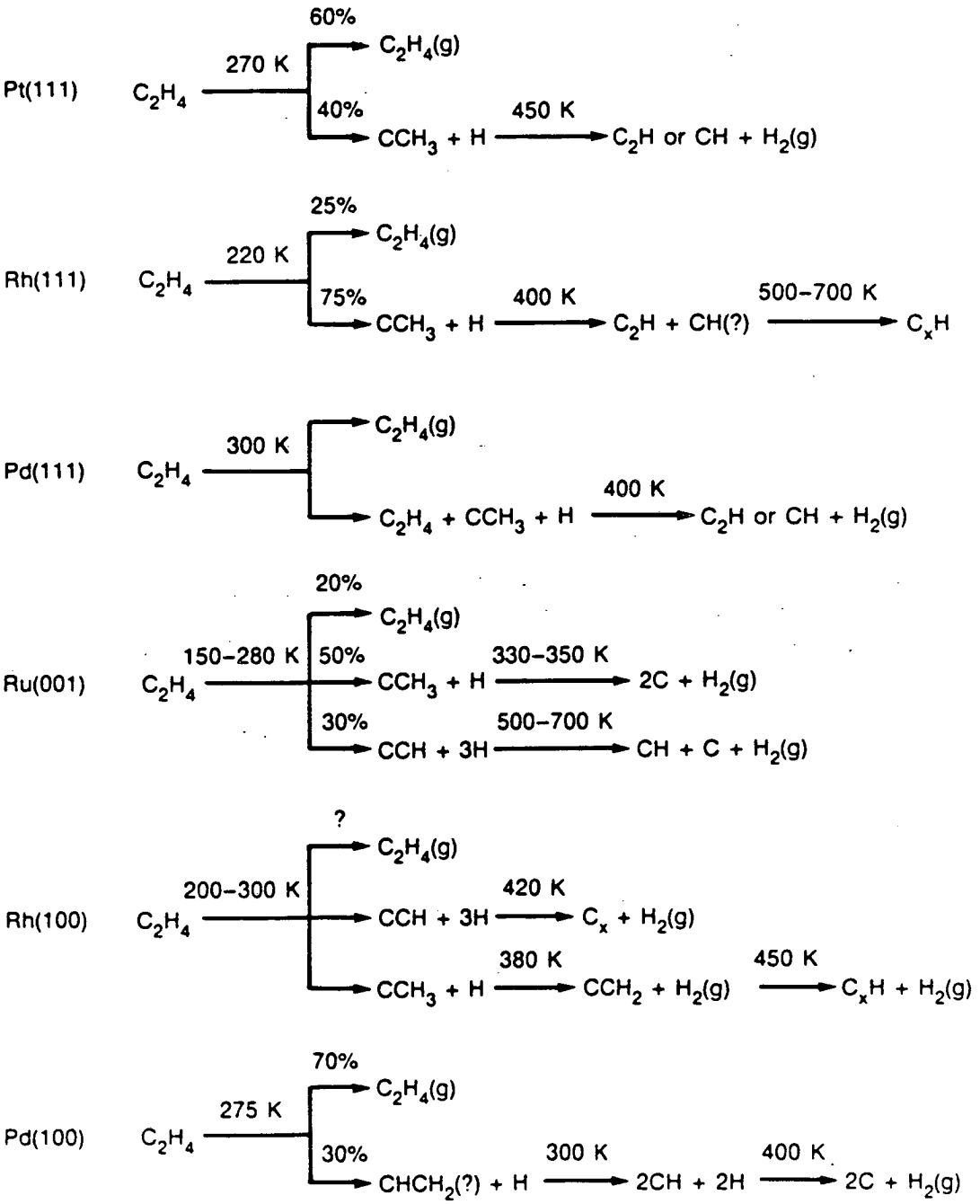

XBL 8610-4104 A

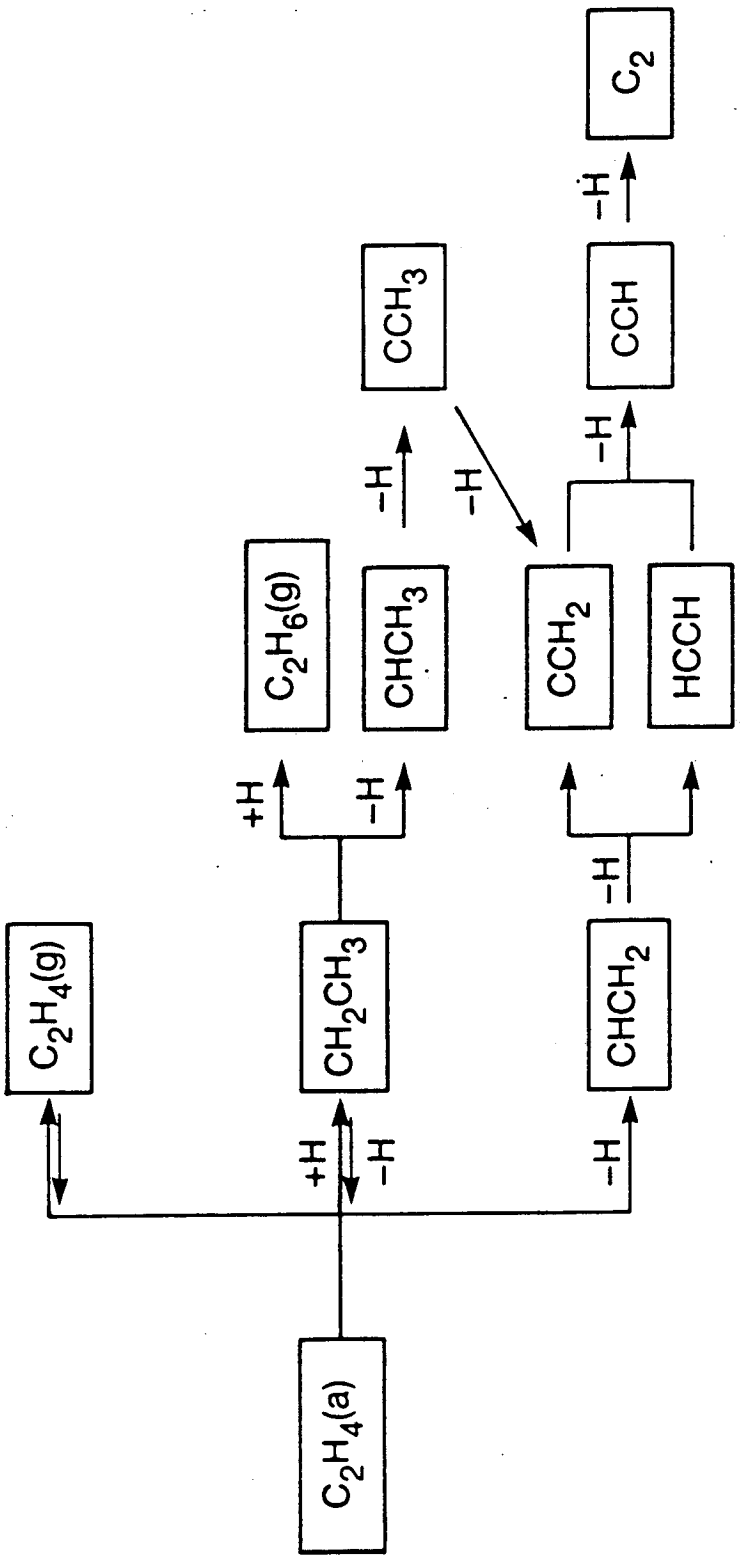
$C_2H_4(a)$
$C_2H_4(g)$
CH_2CH_3
$CHCH_2$
$C_2H_6(g)$
$CHCH_3$
CCH_2
$HCCH$
CCH_3
CCH
C_2
+H
−H
XBL 882-9560

LAWRENCE BERKELEY LABORATORY
TECHNICAL INFORMATION DEPARTMENT
UNIVERSITY OF CALIFORNIA
BERKELEY, CALIFORNIA 94720